Comparison of Rip Current Hazard Likelihood Forecasts with Observed Rip Current Speeds

MELISSA MOULTON

Applied Physics Laboratory, University of Washington, Seattle, Washington

GREGORY DUSEK

Center for Operational Oceanographic Products and Services, National Ocean Service, National Oceanic and Atmospheric Administration, Silver Spring, Maryland

STEVE ELGAR AND BRITT RAUBENHEIMER

Woods Hole Oceanographic Institution, Woods Hole, Massachusetts

(Manuscript received 14 June 2017, in final form 31 July 2017)

ABSTRACT

Although rip currents are a major hazard for beachgoers, the relationship between the danger to swimmers and the physical properties of rip current circulation is not well understood. Here, the relationship between statistical model estimates of hazardous rip current likelihood and in situ velocity observations is assessed. The statistical model is part of a forecasting system that is being made operational by the National Weather Service to predict rip current hazard likelihood as a function of wave conditions and water level. The temporal variability of rip current speeds (offshore-directed currents) observed on an energetic sandy beach is correlated with the hindcasted hazard likelihood for a wide range of conditions. High likelihoods and rip current speeds occurred for low water levels, nearly shore-normal wave angles, and moderate or larger wave heights. The relationship between modeled hazard likelihood and the frequency with which rip current speeds exceeded a threshold was assessed for a range of threshold speeds. The frequency of occurrence of high (threshold exceeding) rip current speeds is consistent with the modeled probability of hazard, with a maximum Brier skill score of 0.65 for a threshold speed of 0.23 m s^{-1}, and skill scores greater than 0.60 for threshold speeds between 0.15 and 0.30 m s^{-1}. The results suggest that rip current speed may be an effective proxy for hazard level and that speeds greater than ~0.2 m s^{-1} may be hazardous to swimmers.

1. Introduction

Rip currents are responsible for tens of thousands of rescues and hundreds of deaths per year at beaches worldwide (Klein et al. 2003; Hartmann 2006; Scott et al. 2007, 2009; Gensini and Ashley 2010; SLSA 2010; Brander and MacMahan 2011; Brighton et al. 2013; USLA 2015). Alongshore variations in wave breaking drive rip current circulation patterns that vary from fixed closed circulation cells to transient jets extending several surfzone widths offshore (MacMahan et al. 2006; Dalrymple et al. 2011; Castelle et al. 2016a; and references therein). The speed and parcel trajectories in rip current circulation patterns are modulated by wave height, direction, and directional spread, along with mean water level, morphology, and coastal currents (MacMahan et al. 2006; Dalrymple et al. 2011; Castelle et al. 2016a; and references therein). The hazard to beachgoers associated with rip currents has been investigated through comparisons of lifeguard visual observations and rescue statistics with measured environmental conditions, including wave properties, tidal elevation, wind speed, and morphology (Lushine 1991; Lascody 1998; Engle et al. 2002; Scott et al. 2007, 2009; Houser et al. 2011; Dusek et al. 2011; Dusek and Seim 2013a). In addition, the effectiveness of escape strategies of swimmers caught in rip currents has been tested in several field and numerical studies (Miloshis and Stephenson 2011; McCarroll et al. 2014, 2015; van Leeuwen et al. 2016; Castelle et al. 2016b). However, little is known about how the hazard to swimmers is related to the physical characteristics of rip current

Corresponding author: Melissa Moulton, mmoulton@apl.uw.edu

DOI: 10.1175/WAF-D-17-0076.1

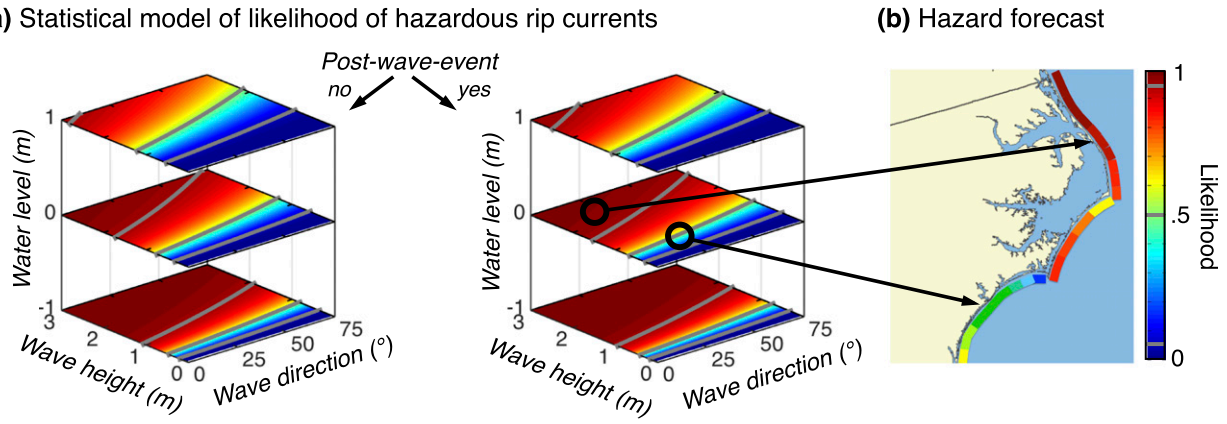

FIG. 1. (a) Statistical model based on lifeguard observations of estimates of the likelihood of hazardous rip currents (color contours; scale on the right and gray contours at 0.05, 0.50, and 0.95) as a function of water level (vertical axes), significant wave height and mean wave direction (horizontal axes), and a binary post-wave-event variable (left = no and right = yes plots). (b) Hazard likelihood is predicted using forecasted wave and water-level inputs for specific times and locations. In an example forecast for North Carolina, hazard likelihood (multicolored band along ~500 km of coastline) varies along the coast with spatially varying wave properties [e.g., circles in (a) have different wave heights and directions].

circulation patterns, including mean speeds, high-frequency pulses, and Lagrangian trajectories (Drozdzewski et al. 2012, 2015; Scott et al. 2014; McCarroll et al. 2015; Castelle et al. 2016a).

A statistical model of the likelihood of hazardous rip currents based on lifeguard observations is being made operational as part of a National Oceanic and Atmospheric Administration National Weather Service (NOAA NWS) rip current hazard forecasting system (Dusek and Seim 2013b; Dusek et al. 2014; Churma et al. 2017). The model estimates the likelihood of hazardous rip currents, defined as rip currents of sufficient strength to cause swimmer distress, as a function of wave properties and water level. The model has skill hindcasting independent lifeguard hazard estimates and is consistent with rescue statistics at several locations (Dusek et al. 2014), but it is not known how the modeled hazard likelihood is related to physical characteristics of rip current circulation. Here, in situ velocity observations on an energetic sandy beach in Duck, North Carolina, are used to investigate the relationship between modeled rip current hazard likelihood and observed rip current speed.

2. Forecast model

The NOAA NWS probabilistic rip current forecast model is based on a logistic regression of in situ wave and water-level observations with lifeguard estimates of rip current intensity in Kill Devil Hills, North Carolina (Dusek and Seim 2013b). The hazard likelihood model is being validated and trained at several additional locations ahead of the anticipated transition to operations at the NWS in 2019 (Churma et al. 2017). The model inputs are significant wave height and mean wave direction (relative to shore normal), mean water level, and a binary post-wave-event variable (Fig. 1a). Bathymetric observations rarely are available, and thus the post-wave-event variable is included as a proxy for the presence of the rip current–favorable bathymetry that often occurs following large waves (e.g., Wright and Short 1984; Garnier et al. 2008): set to 1 (yes) for the 72 h following the peak of a moderate wave event (>1-m height) and 0 (no) at other times. Hazard likelihood is greatest during periods of lower water level, larger wave height, closer to shore-normal wave direction, and in the 72 h following a wave event (post–wave event = yes) (Fig. 1a). In operations, the model is forced by waves and water levels at the 5-m-depth contour from the Nearshore Wave Prediction System (NWPS), an operational wave [Simulating Waves Nearshore (SWAN)] and water-level [Advanced Circulation (ADCIRC) Model] modeling system run at NWS Weather Forecast Offices across the coastal United States (Dusek et al. 2014; van der Westhuysen 2013, 2017). The forecast model output is an hourly likelihood of hazardous rip currents every ~1 km along the U.S. coast (Fig. 1b).

3. Field observations

Currents (Fig. 2, black arrows) were observed using bottom-mounted acoustic Doppler velocimeters and profilers on a long, straight beach near Duck for a total of 10 weeks in 2012 and 2013 at 8–15 locations (Fig. 2, circles), spanning 100–300 m alongshore and from the shoreline to ~3-m depth. In 2012, five experiments were conducted in which single channels were dredged across

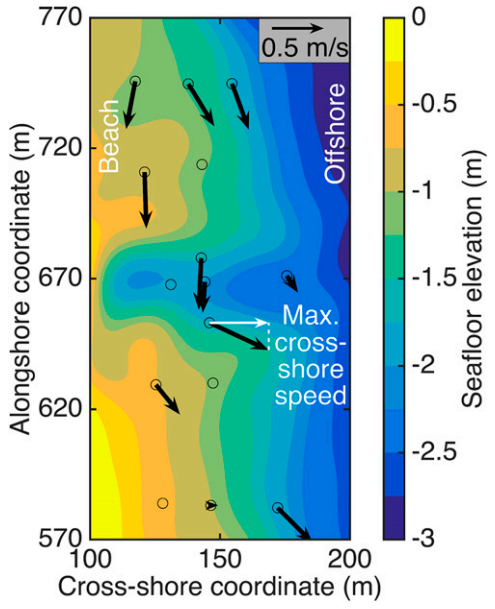

FIG. 2. Observed currents (black arrows; scale in upper right), estimated rip current speed (maximum cross-shore component; white arrow), and bathymetry (color contours; scale on the right) for 1800 EDT 25 Jul 2012. Arrays were similar at other times in 2012 and 2013 (not shown), and the bathymetry varied from channeled (artificial and natural channels were similar) to nearly alongshore uniform (e.g., shore-parallel contours similar to those near $570 < y < 620$ m).

the surfzone using landing-craft propellers to create bathymetry that initially was favorable to rip currents (Moulton et al. 2014, 2017). The subsequent evolution of the bathymetry included migration and infill of the channels. Arrays of current meters and profilers centered on the channel were deployed 1–2 days after each dredging (28 June, and 7, 18, 24, and 30 July; numbered at the top of Fig. 3a). In 2013 natural bathymetry (not artificially modified) varied from alongshore uniform with a shore-parallel sandbar to alongshore inhomogeneous with channeled or crescentic sandbars. Natural channels were similar to the artificial dredged channels (Fig. 2). Wave properties in ~5-m depth were measured a few hundred meters alongshore of the surfzone sensor arrays by a long-term observing system maintained by the U.S. Army Corps of Engineers Field Research Facility (http://frf.usace.army.mil/frf.shtml) (Hanson et al. 2009). Significant wave heights, energy-weighted wave angles, and centroidal wave periods were computed for a frequency band from 0.05 to 0.30 Hz (Kuik et al. 1988). Significant wave heights ranged from 0.3 to 3.5 m, and wave incidence angles ranged from −25° to 45° relative to shore normal (positive is from clockwise of shore normal) (Figs. 3b, 3c, 3f, 3g). Centroidal wave periods ranged from 5 to 11 s (not shown). The mean water level was measured a few hundred meters alongshore of the surfzone sensor arrays with a NOAA water-level station in 6-m depth (Figs. 3d, 3h). The mean water level is primarily modulated by the tides, and includes smaller contributions from other processes, including storm surge and shelf waves.

Rip current jets are relatively narrow [$O(10)$ m], and it is not known a priori where they appear in the sensor arrays. Thus, a proxy for the rip current speed at each time is defined as the maximum hour-averaged Eulerian cross-shore current (white arrow in Fig. 2, red curves in Fig. 3) (Moulton et al. 2017). Despite the relatively dense sensor spacing, the strongest rip current jet sometimes may have been between the sensors (Moulton et al. 2017). Some sensors were not submerged during the passage of wave troughs at low tide or were buried as the channel morphology evolved (Fig. 2, circles with no current vectors), and the fixed in situ arrays did not resolve particle trajectories or the cross-shore extent of rip currents. Occasionally, the fastest cross-shore flows may have been a near-bottom return flow (undertow) rather than a rip current jet.

4. Results

The forecast model was forced with hourly observed mean water level, significant wave height and direction, and proximity to a moderate wave event (gray shading in Figs. 3b, 3f) for the datasets collected in 2012 (Figs. 3b–d) and 2013 (Figs. 3f–h). The temporal variability of the modeled rip current hazard likelihood (blue curves in Figs. 3a, 3e) is similar to the variability in the observed rip current speed (maximum offshore-directed flow speed across all sensors) (red curves in Figs. 3a, 3e). Times when the strongest rip current speeds (up to $\sim 1\,\mathrm{m\,s^{-1}}$) were observed coincide with high hindcasted hazard likelihoods, and the sensitivity of hazard and speed to wave height, wave angle, and water level is similar (Fig. 3). High rip current speeds occurred at low water levels and for larger and more nearly shore-normal waves (Figs. 3, 4), consistent with the statistical model behavior (Figs. 1a, 3, 4). However, sometimes high hazard likelihoods and rip current speeds also occurred with moderate wave heights (Fig. 4, 19–23 July), and some of the highest likelihoods corresponded to speeds that were moderate relative to the largest observed speeds (Fig. 4, 25–27 July). During some instances of oblique wave incidence, rip current speeds were small, whereas modeled hazard likelihood was high (Fig. 4, 27–28 July).

The relationship between bathymetric variability and the post-wave-event variable, intended to be a proxy for bathymetry favorable to rip currents, was not assessed

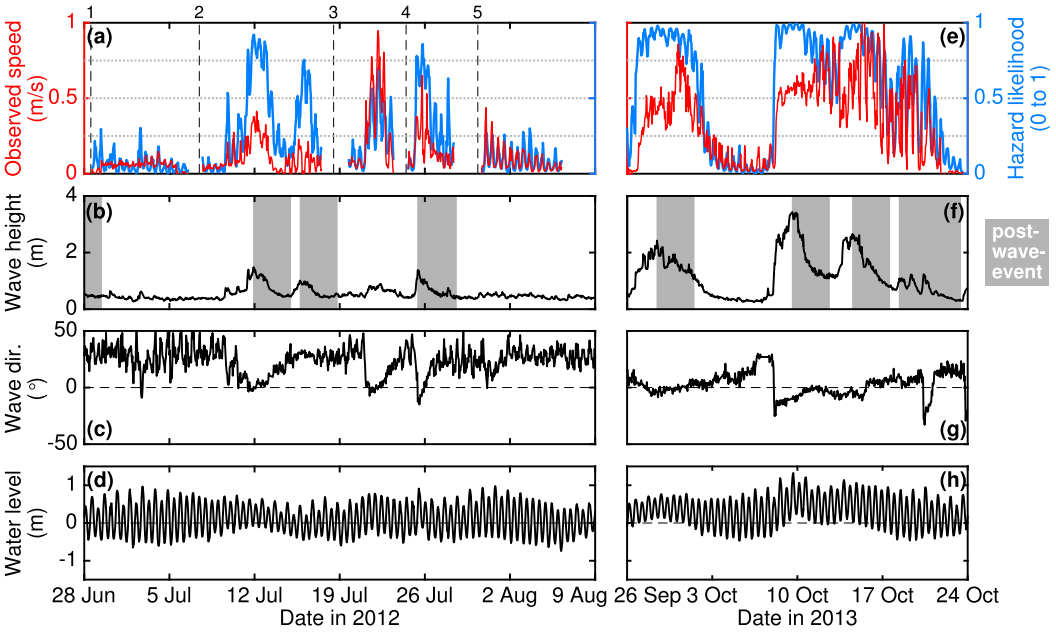

FIG. 3. (a),(e) Observed rip current speed (red; left-hand y axis) and modeled likelihood of hazard (blue; right-hand y axis); (b),(f) observed significant wave height (72-h post–wave event shaded gray); (c),(g) mean wave direction (relative to shore normal); and (d),(h) water level relative to mean sea level vs date in (left) 2012 and (right) 2013. Velocity and bathymetry sensors were removed and redeployed at five times when single channels were dredged in 2012 [numbered dashed vertical lines in (a)].

because in 2012 the bathymetry was artificial (Fig. 4d) and in 2013 bathymetric observations were infrequent. However, the presence of artificial or unknown bathymetry is not expected to have a large impact on the results, as likelihood hindcasts were only weakly sensitive to the post-event variable (cf. left with right figures in Fig. 1a, and compare dark with light blue curves in Fig. 4a).

There are no instances with low hazard likelihood and high observed speeds, and all instances with large observed speeds have a high likelihood of hazard (Fig. 5a). To compare the observations with the model more quantitatively, the frequency with which observed rip current speeds (Figs. 3a, 4a, 5a) exceeded a threshold U_t is compared with model hazard likelihood. Binary time series of observed threshold exceedance were computed for $0.10 \le U_t \le 0.60\,\mathrm{m\,s^{-1}}$ in $0.01\,\mathrm{m\,s^{-1}}$ increments. For each value of U_t, the binary observations of exceedance (1 if speed $> U_t$, 0 if speed $< U_t$) were averaged within 10 modeled likelihood bins (between 0 and 1) (Fig. 5b). If the forecast model had perfect reliability, then high speeds (defined as exceeding the threshold) would occur with a frequency equal to the forecasted hazard likelihood (Fig. 5b, dashed 1:1 line).

In addition, for each threshold speed, a Brier skill score (BSS) was computed (Fig. 6), where $\mathrm{BSS} = 1 - \mathrm{BS/BS_{ref}}$, where BS is the Brier score (root-mean-square difference of the observed frequencies and forecast likelihoods) and $\mathrm{BS_{ref}}$ is a reference Brier score equal to the average of the binary observations (a climatological value; Fig. 5b, symbols on the vertical axis) (Wilks 1995, 2006). Positive BSS values indicate positive skill, with $\mathrm{BSS} = 1$ ($\mathrm{BS/BS_{ref}} = 0$) for perfect skill, $\mathrm{BSS} = 0$ ($\mathrm{BS/BS_{ref}} = 1$) for zero skill, and $\mathrm{BSS} < 0$ ($\mathrm{BS/BS_{ref}} > 1$) for negative skill (which is unbounded). For each threshold speed, a mean bias error (MBE, the mean signed deviation of the observed frequency of events from the forecasted frequency) was computed (Fig. 5b, compare symbols with 1:1 line). The results are not sensitive to the number of threshold speeds or bins.

The maximum BSS is 0.65 and the minimum |MBE| is ~2% for a threshold speed $U_t = 0.23\,\mathrm{m\,s^{-1}}$, indicating that the forecast provides a 65% improvement over using the climatological observation (Fig. 6) and is well calibrated (Fig. 5b). The refinement distribution (Fig. 5c) indicates that there are many instances with extreme forecast probabilities (closer to 0 or 1 than to 0.5), suggesting high confidence in the reliability estimates (Fig. 5b) (Wilks 1995, 2006). The minimum BS value corresponding to the maximum BSS is 0.08. The skills reported here are similar to previous tests of the forecast model (Dusek and Seim 2013b; Dusek et al. 2014). Peak BSS values vary by <0.01 if the post-event variable is forced to either 0 or 1. BSS and MBE values

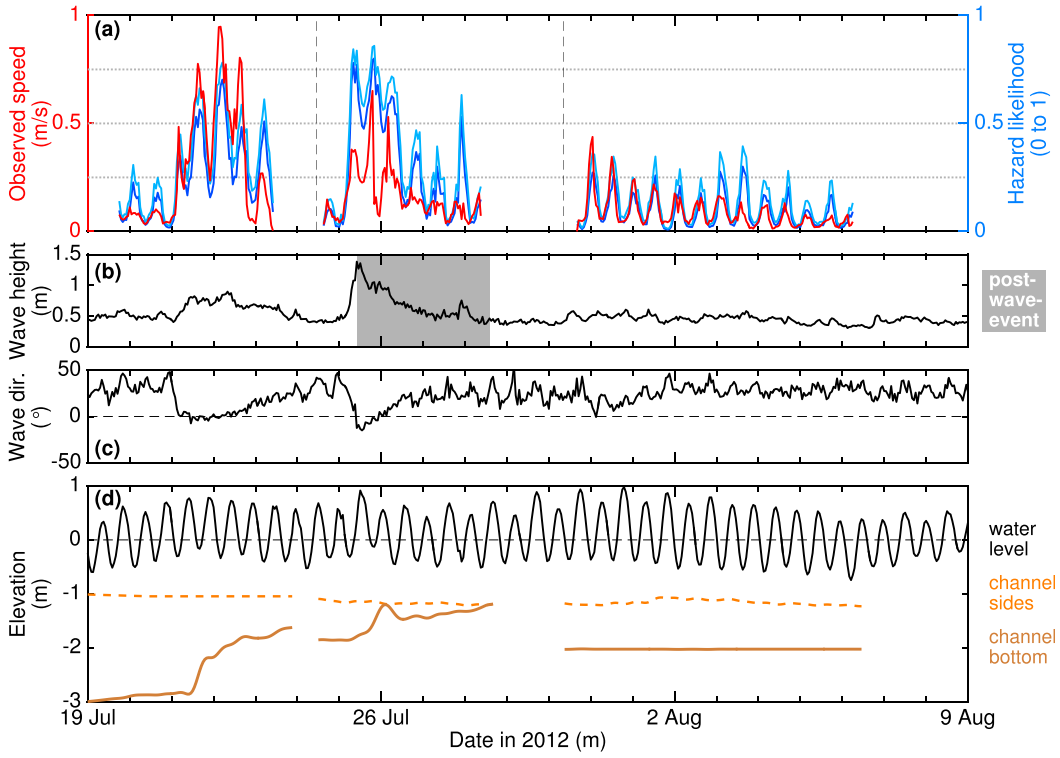

FIG. 4. (a) Observed rip current speed (red; left-hand *y* axis) and modeled likelihood of hazard (right-hand *y* axis) for post-wave-event variable 0 (darker blue) and 1 (lighter blue), (b) observed significant wave height in ~5-m depth (72-h post–wave event shaded gray), (c) mean wave direction (relative to shore normal) in ~5-m depth, and (d) elevation (relative to mean sea level) of sea surface (black), seafloor on channel sides (dashed orange), and seafloor in deepest part of channel (brown) vs date in 2012.

are relatively insensitive to the threshold speed for $0.15 \leq U_t \leq 0.30\,\mathrm{m\,s^{-1}}$, with $0.60 < \mathrm{BSS} < 0.65$ and $2\% < |\mathrm{MBE}| < 10\%$. Although the model exhibits positive skill for a wide range of threshold speeds (Fig. 6), for threshold speeds outside of the range from 0.15 to $0.30\,\mathrm{m\,s^{-1}}$, the forecast increasingly underpredicts or overpredicts the probability of observed high speeds (Fig. 5b), and the forecast skill decreases (Fig. 6). For $U_t = 0.1\,\mathrm{m\,s^{-1}}$, BSS = 0.40 (Fig. 6) and the model underpredicts high flow speeds by 15% (Fig. 5, MBE = 15%). For $U_t = 0.4\,\mathrm{m\,s^{-1}}$, BSS = 0.40 (Fig. 6) and the model overpredicts high flow speeds by 15% (Fig. 5, MBE = −15%).

5. Discussion

Quantifying the relationship between physical properties of rip current circulation and hazard to swimmers is important for public safety, but hazard forecasts previously had not been compared with observed rip current speeds. Swimmers may become exhausted and panic if they are not able to swim against a fast current or are carried away from shore quickly (Drozdzewski et al. 2012, 2015), consistent with the results here that suggest the likelihood of hazard increases with increasing frequency of rip current speeds exceeding a threshold of $\sim 0.2\,\mathrm{m\,s^{-1}}$ (Fig. 5). The similarity between the observed speeds and hindcasted likelihoods (Figs. 3a, 3e, 4a) suggests that the conditions that lead to strong rip currents are similar to the conditions for which lifeguards are most likely to identify the presence of rip currents that are hazardous to swimmers (Fig. 1). High speeds and high hazard likelihoods occurred for wave angles close to shore normal and for large ratios of wave height to water level, consistent with the dynamics of rip currents generated by wave breaking on local bathymetric variations (Moulton et al. 2017).

Differences between the observations and model may result from the inability to include bathymetry as a direct model input, uncertainties in the hazard model, errors in estimating the maximum rip current speed from fixed sensors, and the assumption that speed alone is a sufficient proxy for hazard to beachgoers. Previous studies suggest that rip current circulation pattern type also may be an important indicator of hazard. For example, the frequency of ejection of floating objects from

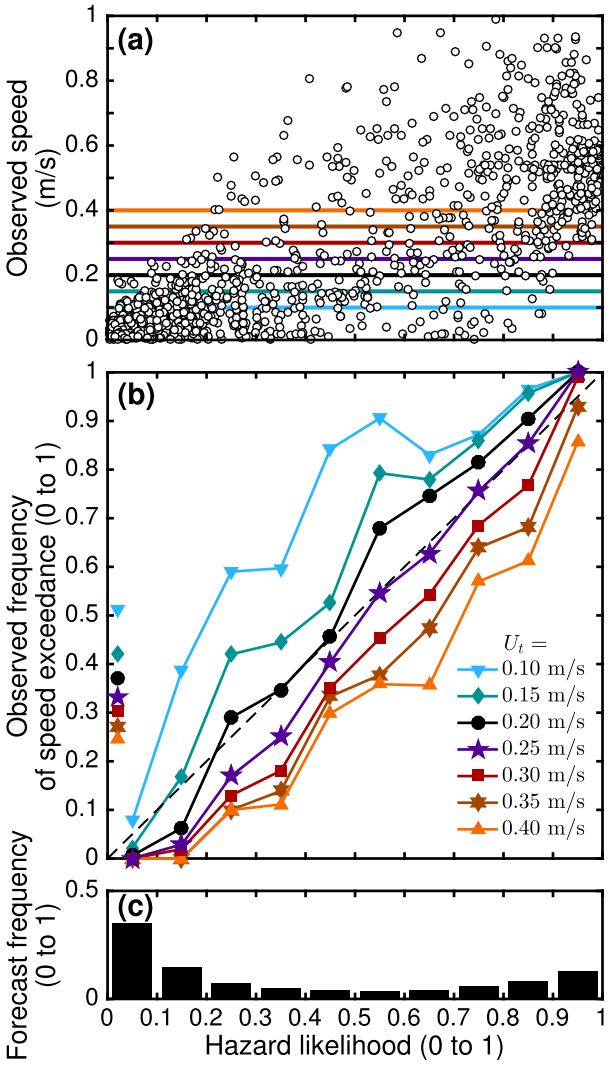

FIG. 5. (a) Observed rip current speed vs modeled likelihood of hazardous rip currents (0–1) for different threshold speeds (horizontal lines). (b) Reliability diagram: observed binned exceedance frequency for a range U_t (symbols connected by colored lines; values given in the legend) vs model hazard likelihood. Mean of binary observations before binning (climatological value) shown with symbols along the vertical axis. The 1:1 line (dashed line) indicates perfect reliability. (c) Refinement distribution: relative frequency of binned forecast likelihood values vs likelihood.

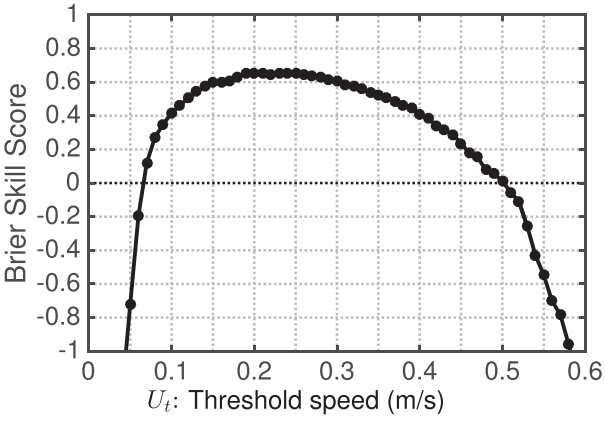

FIG. 6. BSS vs U_t.

the surfzone (surfzone "exits") is expected to be linked closely with swimmer hazard and varies substantially in different rip current systems (Reniers et al. 2009; MacMahan et al. 2010; Scott et al. 2014; Pitman et al. 2016), including rip currents formed by local (MacMahan et al. 2006) and offshore (Long and Özkan-Haller 2005) bathymetric variations, or by short-crested wave breaking (Suanda and Feddersen 2015). The relationship between mean rip current speed and surfzone exits is complex, partly as a result of the wide range of circulation pattern types, the range of time scales of rip current variability, spatial and temporal changes in the surfzone width, and the presence of Stokes drift (Scott et al. 2014). Understanding of these factors could be improved by comparing the hazard model with observations of rip current speed at a broader range of geographic locations, including sites where transient rip currents and rip currents formed by offshore bathymetry, such as submarine canyons, are prevalent (e.g., on the southern California coast; Long and Özkan-Haller 2005).

Validation and calibration of the forecast model with lifeguard observations is ongoing at multiple new locations with a range of wave, tide, and bathymetric conditions, and resulting rip current types. Future development of the hazardous rip current forecasting system will be informed by improved understanding of the relationships between hazard likelihood, speed, and other characteristics of rip current circulation, including high-frequency pulses and Lagrangian trajectories.

6. Conclusions

National Weather Service forecasts of rip current hazard likelihoods are consistent with lifeguard estimates of the hazard. Here, hourly rip current speeds observed for a range of incident wave conditions on a long, straight ocean beach were compared with hazard forecasts. Both strong observed rip current speeds and high hazard likelihoods were associated with low tidal elevations, shore-normal wave incidence, and moderate or larger wave heights. The hazard likelihood model has significantly higher skill than a prediction based on climatology, with Brier skill score > 0.60 and mean bias errors $< 10\%$ when compared with observed occurrences of rip currents speeds greater than a range of possible thresholds from 0.15 to 0.30 $\mathrm{m\,s^{-1}}$ (maximum

skill score = 0.65 and minimum bias ~2% for speed ~0.23 m s^{-1}). The comparisons of modeled hazard likelihood with observed rip current speeds suggest that exceedance of a speed threshold may be an effective proxy for swimmer hazard associated with rip currents, and that speeds greater than approximately 0.2 m s^{-1} may be hazardous.

Acknowledgments. We thank the PVLAB and FRF field teams for deploying, maintaining, and recovering the arrays of sensors in the surfzone under difficult conditions. Incident wave heights and directions, bathymetric surveys, heavy equipment operation, and logistical support were provided by the Field Research Facility, Coastal Observations and Analysis Branch, U.S. Army Corps of Engineers, Duck, North Carolina. Water-level observations were provided by the National Oceanic and Atmospheric Administration Center for Operational Oceanographic Products and Services. Funding was provided by the National Science Foundation (1232910, 1332705, and 1536365), and by National Security Science and Engineering and Vannevar Bush Faculty Fellowships funded by the assistant secretary of Defense for Research and Engineering. Data are available via e-mail to the corresponding author.

REFERENCES

Brander, R. W., and J. H. MacMahan, 2011: Future challenges for rip current research and community outreach. *Rip Currents: Beach Safety, Physical Oceanography, and Wave Modeling*, S. Leatherman and J. Fletemeyer, Eds., CRC Press, 1–29.

Brighton, B., S. Sherker, R. Brander, M. Thompson, and A. Bradstreet, 2013: Rip current related drowning deaths and rescues in Australia. *Nat. Hazards Earth Syst. Sci.*, **13**, 1069–1075, doi:10.5194/nhess-13-1069-2013.

Castelle, B., T. Scott, R. W. Brander, and R. J. McCarroll, 2016a: Rip current types, circulation and hazard. *Earth-Sci. Rev.*, **163**, 1–21, doi:10.1016/j.earscirev.2016.09.008.

——, R. J. McCarroll, R. W. Brander, T. Scott, and B. Dubarbier, 2016b: Modelling the alongshore variability of optimum rip current escape strategies on a multiple rip-channelled beach. *Nat. Hazards*, **81**, 663–686, doi:10.1007/s11069-015-2101-3.

Churma, M. E., and Coauthors, 2017: Observation methodologies for NOAA operational rip current forecast models. *15th Symp. on the Coastal Environment*, Seattle, WA, Amer. Meteor. Soc., 2.3, https://ams.confex.com/ams/97Annual/webprogram/Paper315894.html.

Dalrymple, R. A., J. H. MacMahan, A. J. H. M. Reniers, and V. Nelko, 2011: Rip currents. *Annu. Rev. Fluid Mech.*, **43**, 551–581, doi:10.1146/annurev-fluid-122109-160733.

Drozdzewski, D., and Coauthors, 2012: Surveying rip current survivors: Preliminary insights into the experiences of being caught in rip currents. *Nat. Hazards Earth Syst. Sci.*, **12**, 1201–1211, doi:10.5194/nhess-12-1201-2012.

——, A. Roberts, D. Dominey-Howes, and R. Brander, 2015: The experiences of weak and non-swimmers caught in rip currents at Australian beaches. *Aust. Geogr.*, **46**, 15–32, doi:10.1080/00049182.2014.953735.

Dusek, G., and H. Seim, 2013a: Rip current intensity estimates from lifeguard observations. *J. Coastal Res.*, **29**, 505–518, doi:10.2112/JCOASTRES-D-12-00117.1.

——, and ——, 2013b: A probabilistic rip current forecast model. *J. Coastal Res.*, **289**, 909–925, doi:10.2112/JCOASTRES-D-12-00118.1.

——, ——, J. Hanson, and D. Elder, 2011: Analysis of rip current rescues at Kill Devil Hills, North Carolina. *Rip Currents: Beach Safety, Physical Oceanography and Wave Modeling*, S. Leatherman and J. Fletemeyer, Eds., CRC Press, 59–86.

——, A. Van der Westhuysen, A. Gibbs, D. King, S. Kennedy, H. Seim, and D. Elder, 2014: Coupling a rip current forecast model to the nearshore wave prediction system. *12th Symp. on the Coastal Environment*, Atlanta, GA, Amer. Meteor. Soc., 3.2, https://ams.confex.com/ams/94Annual/webprogram/Paper238859.html.

Engle, J., J. MacMahan, R. J. Thieke, D. M. Hanes, and R. G. Dean, 2002: Formulation of a rip current predictive index using rescue data. *Proc. 15th Annual Natl. Conf. on Beach Preservation Technology*, Florida Shore and Beach Preservation Association, http://www.nws.noaa.gov/ripcurrents/resources/Engle2002.pdf.

Garnier, R., D. Calvete, A. Falqués, and N. Dodd, 2008: Modelling the formation and the long-term behavior of rip channel systems from the deformation of a longshore bar. *J. Geophys. Res.*, **113**, C07053, doi:10.1029/2007JC004632.

Gensini, V. A., and W. S. Ashley, 2010: An examination of rip current fatalities in the United States. *Nat. Hazards*, **54**, 159–175, doi:10.1007/s11069-009-9458-0.

Hanson, J. L., H. C. Friebel, and K. K. Hathaway, 2009: Coastal wave energy dissipation: Observations and STWAVE-FP performance. *11th Int. Workshop on Wave Hindcasting and Forecasting and Second Coastal Hazards Symp.*, Halifax, NS, Canada, U.S. Army, Environment Canada, and JCOMM, http://waveworkshop.org/11thWaves/Papers/HansonEtAl_Halifax.pdf.

Hartmann, D., 2006: Drowning and beach-safety management (BSM) along the Mediterranean beaches of Israel—A long-term perspective. *J. Coastal Res.*, **22**, 1505–1514, doi:10.2112/05-0497.1.

Houser, C., G. Barrett, and D. Labude, 2011: Alongshore variation in the rip current hazard at Pensacola Beach, Florida. *Nat. Hazards*, **57**, 501–523, doi:10.1007/s11069-010-9636-0.

Klein, A. H. da F., G. G. Santana, F. L. Diehl, and J. T. de Menezes, 2003: Analysis of hazards associated with sea bathing: Results of work in oceanic beaches of Santa Catarina State, Southern Brazil. *J. Coastal Res.*, **35**, 107–116, http://www.jstor.org/stable/40928754.

Kuik, A., G. van Vledder, and L. Holthuijsen, 1988: A method for the routine analysis of pitch-and-roll buoy wave data. *J. Phys. Oceanogr.*, **18**, 1020–1034, doi:10.1175/1520-0485(1988)018<1020:AMFTRA>2.0.CO;2.

Lascody, R. L., 1998: East Central Florida rip current program. *Natl. Wea. Dig.*, **22** (2), 25–30.

Long, J. W., and H. T. Özkan-Haller, 2005: Offshore controls on nearshore rip currents. *J. Geophys. Res.*, **110**, C12007, doi:10.1029/2005JC003018.

Lushine, J. B., 1991: A study of rip current drownings and related weather factors. *Natl. Wea. Dig.*, **16** (3), 13–19.

MacMahan, J. H., E. B. Thornton, and A. J. H. M. Reniers, 2006: Rip current review. *Coastal Eng.*, **53**, 191–208, doi:10.1016/j.coastaleng.2005.10.009.

——, and Coauthors, 2010: Mean Lagrangian flow behavior on an open coast rip-channeled beach: A new perspective. *Mar. Geol.*, **268**, 1–15, doi:10.1016/j.margeo.2009.09.011.

McCarroll, R. J., R. W. Brander, J. H. MacMahan, I. L. Turner, A. J. H. M. Reniers, J. A. Brown, A. Bradstreet, and S. Sherker, 2014: Evaluation of swimmer-based rip current escape strategies. *Nat. Hazards*, **71**, 1821–1846, doi:10.1007/s11069-013-0979-1.

——, B. Castelle, R. W. Brander, and T. Scott, 2015: Modelling rip current flow and bather escape strategies across a transverse bar and rip channel morphology. *Geomorphology*, **246**, 502–518, doi:10.1016/j.geomorph.2015.06.041.

Miloshis, M., and W. J. Stephenson, 2011: Rip current escape strategies: Lessons for swimmers and coastal rescue authorities. *Nat. Hazards*, **59**, 823–832, doi:10.1007/s11069-011-9798-4.

Moulton, M., S. Elgar, and B. Raubenheimer, 2014: Improving the time resolution of surfzone bathymetry using in situ altimeters. *Ocean Dyn.*, **64**, 755–770, doi:10.1007/s10236-014-0715-8.

——, ——, ——, J. C. Warner, and N. Kumar, 2017: Rip currents and alongshore flows in single channels dredged in the surf zone. *J. Geophys. Res. Oceans*, **122**, 3799–3816, doi:10.1002/2016JC012222.

Pitman, S., S. L. Gallop, I. D. Haigh, G. Masselink, and R. Ranasinghe, 2016: Wave breaking patterns control rip current flow regimes and surfzone retention. *Mar. Geol.*, **382**, 176–190, doi:10.1016/j.margeo.2016.10.016.

Reniers, A. J. H. M., J. H. MacMahan, E. B. Thornton, T. P. Stanton, M. Henriquez, J. W. Brown, J. A. Brown, and E. Gallagher, 2009: Surf zone surface retention on a rip-channeled beach. *J. Geophys. Res.*, **114**, C10010, doi:10.1029/2008JC005153.

Scott, T., P. Russell, G. Masselink, A. Wooler, and A. Short, 2007: Beach rescue statistics and their relation to nearshore morphology and hazards: A case study for southwest England. *J. Coastal Res.*, **50**, 1–6.

——, ——, ——, and ——, 2009: Rip current variability and hazard along a macro-tidal coast. *J. Coastal Res.*, **56**, 895–899.

——, G. Masselink, M. J. Austin, and P. E. Russell, 2014: Controls on macrotidal rip current circulation and hazard. *Geomorphology*, **214**, 198–215, doi:10.1016/j.geomorph.2014.02.005.

SLSA, 2010: Preventing coastal drowning deaths in Australia. National Coastal Safety Rep., Surf Life Saving Australia, 22 pp.

Suanda, S. H., and F. Feddersen, 2015: A self-similar scaling for cross-shelf exchange driven by transient rip currents. *Geophys. Res. Lett.*, **42**, 5427–5434, doi:10.1002/2015GL063944.

USLA, 2015: National lifesaving statistics. United States Lifesaving Association, http://arc.usla.org/Statistics/current.asp?Statistics=5.

van der Westhuysen, A. J., and Coauthors, 2013: Development and validation of the Nearshore Wave Prediction System. *11th Symp. on the Coastal Environment*, Austin, TX, Amer. Meteor. Soc., 4.5, https://ams.confex.com/ams/93Annual/webprogram/Paper222877.html.

——, and Coauthors, 2017: National deployment of the Nearshore Wave Prediction System for marine hazard guidance. *15th Symp. on the Coastal Environment*, Seattle, WA, Amer. Meteor. Soc., J3.2, https://ams.confex.com/ams/97Annual/webprogram/Paper316096.html.

van Leeuwen, B. R., R. J. McCarroll, R. W. Brander, I. L. Turner, H. E. Power, and A. J. Bradstreet, 2016: Examining rip current escape strategies in non-traditional beach morphologies. *Nat. Hazards*, **81**, 145–165, doi:10.1007/s11069-015-2072-4.

Wilks, D. S., 1995: *Statistical Methods in the Atmospheric Sciences: An Introduction*. Academic Press, 467 pp.

——, 2006: *Statistical Methods in the Atmospheric Sciences*. 2nd ed. International Geophysics Series, Vol. 91, Academic Press, 627 pp.

Wright, L. D., and A. D. Short, 1984: Morphodynamic variability of surf zones and beaches: A synthesis. *Mar. Geol.*, **56**, 93–118, doi:10.1016/0025-3227(84)90008-2.